J. Phys. B: At. Mol. Opt. Phys. **42** (2009) 114005 (7pp) doi:10.1088/0953-4075/42/11/114005

Implementation of single-photon creation and annihilation operators: experimental issues in their application to thermal states of light

V Parigi[1], **A Zavatta**[1,2] **and M Bellini**[1,2]

[1] European Laboratory for Nonlinear Spectroscopy (LENS), University of Florence, Via N. Carrara 1, 50019 Sesto Fiorentino Firenze, Italy
[2] Istituto Nazionale di Ottica Applicata (INOA-CNR) Largo E. Fermi 6, 50125 Firenze, Italy

E-mail: bellini@inoa.it

Received 16 January 2009, in final form 5 March 2009
Published 15 May 2009
Online at stacks.iop.org/JPhysB/42/114005

Abstract
We have recently realized experimental schemes to implement the action of single-photon creation and annihilation operators onto completely classical and fully incoherent thermal light states (Parigi *et al* 2007 *Science* **317** 1890). By applying alternated sequences of the creation and annihilation operators we observed that the resulting states depend on the order in which the two quantum operators are applied, thus obtaining the most direct experimental test of non-commutativity. Here we provide an extensive and detailed discussion of the main experimental issues related to the realization of these schemes.

(Some figures in this article are in colour only in the electronic version)

1. Introduction

Recently, we succeeded in the realization of an experiment for demonstrating the non-commutativity of creation and annihilation operators [1]. A simplified block diagram of the experiment is depicted in figure 1 and may help to visualize the involved operations. A module for single-photon creation (implemented by conditional parametric down-conversion and denoted by $\hat{a}^{\dagger}$) is placed between two modules for single-photon annihilation (implemented by means of low-reflectivity beam splitters (BS) and denoted by $\hat{a}$). Alternated sequences of the operators were obtained by conditioning upon double clicks from the first/second or second/third modules with a thermal state as the input.

An experimental scheme to directly prove the commutation relation between bosonic annihilation and creation operators has also been proposed very recently [2]. A single-photon interferometer mixing the heralding outputs of the two beam splitters used for photon subtraction is used to realize coherent superpositions of two alternated sequences of the creation and annihilation operators. It has been shown that, depending on the interference outcome, the commutation relation is directly proven, or a highly nonclassical state is produced.

The realization of such single-photon operations in an efficient and faithful way is of high importance both for fundamental studies of quantum physics and for the full engineering of quantum light states. Besides testing the non-commutativity of bosonic creation and annihilation operators [1], we also recently investigated other basic quantum rules, such as the invariance of coherent states under the process of single-photon annihilation [3, 4] or explored the quantum-to-classical transition of light by exciting a coherent state with a single photon [5]. Other groups successfully implemented single-photon subtraction to produce cat-like states of light [6–9] and, in general, to obtain non-Gaussian continuous-variable states, which are predicted to bring definite advantages in several protocols for quantum-enhanced measurements and communication tasks [10–16].

Here we present a detailed analysis of some of the experimental issues involved in the implementation of single-photon creation and annihilation operators, with a special

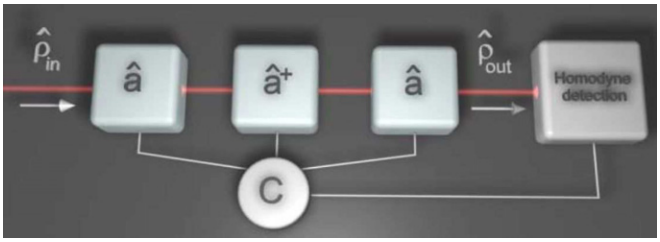

Figure 1. Block diagram of the experiment for the test of non-commutativity between creation and annihilation operators.

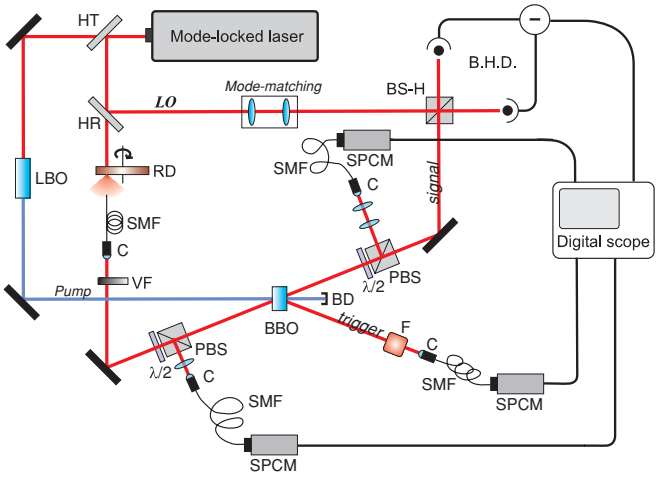

Figure 2. Scheme of the complete experimental setup. Most symbols are defined in the text. BBO indicates the beta barium borate SPDC crystal. The beam splitters for photon subtraction are composed of a half-wave plate ($\lambda/2$) and a polarizing beam splitter (PBS) for accurate adjustments of their transmissivity. C stands for collimating (collecting) optics for single-mode fibres (SMF). SPCM: on/off detector, HT (HR): high-transmissivity (reflectivity) mirror, BD: beam dump.

regard to the application of their sequences onto thermal light states for the test of non-commutativity. These considerations are also valid for more general schemes and should be of help when designing new experiments for the precise generation, manipulation and tomographic analysis of quantum states of light.

2. Experimental setup

The primary laser source of the experimental apparatus shown in figure 2 is a mode-locked Ti:Sa laser (Spectra-Physics Tsunami) emitting 1.5 ps pulses at a repetition rate of 82 MHz. The fundamental beam at 786 nm is frequency doubled in a 9 mm long second-harmonic crystal (LBO: lithium triborate) [17] generating about 300 mW of UV radiation. The UV beam is spatially cleaned by a pin-hole spatial filter in order to be used as the pump for a second nonlinear crystal (BBO: beta barium borate, type-I) to generate spontaneous parametric down-conversion (SPDC). Degenerate SPDC is emitted in two different channels called signal and idler, at a wavelength equal to that of the fundamental laser emission. This allows a simple implementation of homodyne detection for the characterization of the signal state, which is mixed with a strong reference coherent field (the local oscillator, LO, a portion of the laser output) on a 50–50 beam splitter (BS-H). The beam splitter outputs are detected by two photodiodes, whose differential signal is acquired and stored by a digital oscilloscope. Our balanced homodyne apparatus (B.H.D.) works on a pulse-to-pulse basis [18, 19] triggered by on/off detectors (one is placed in the idler/trigger beam for conditional parametric down-conversion). Homodyne measurements are proportional to different field quadratures depending on the relative phase between the LO and the signal. Since the states generated as described below (photon-added or -subtracted thermal states) present no phase dependence, the LO phase is left unlocked in the measurements. It is also important to recall that only the portion of the signal field which is in the same spatiotemporal mode of the LO is effectively analysed by the homodyne detector. Many sequences of quadrature measurements (in principle, with different phase values) are used to completely reconstruct the density matrix of the light state. In the following examples, state reconstruction is performed by making use of the maximum likelihood estimation method [20], which gives the density matrix that most likely represents the measured homodyne data (for details see [21, 22]).

2.1. Adding a single photon to a thermal state

The single-photon-added thermal states, first described by Agarwal and Tara in 1992 [23], are generated in a conditional way by exploiting the parametric amplification at the single-photon level. When no field is injected in the SPDC crystal, a pump photon, due to the crystal nonlinearity, can be converted into two simultaneously generated photons (one in the signal channel and one in the idler one) correlated in frequency and in momentum. The click of the on/off photodetector (an avalanche photodiode which can discern there being at least one photon from no photons) placed in the idler path after narrow spectral and spatial filters (F) is used to conditionally prepare a single photon in a well-defined spatiotemporal mode of the signal channel (further details are given in [24–26]). The probability of the process is proportional to $|g|^2$ where $g = \chi^{(2)}t$ is the parametric gain, $\chi^{(2)}$ being the second-order susceptibility and t the interaction time. On the other hand, if the SPDC crystal is seeded with a state described by the operator $\hat{\rho}$, stimulated emission comes into play, and single-photon excitation of such a state is conditionally obtained [5, 25, 27, 28] when one photon is detected in the idler mode. In the low-gain regime the probability of stimulated emission in the idler channel is proportional to $|g|^2(1+\bar{n})$ where $\bar{n}$ is the mean photon number of the seed state. Thus the ratio between the idler counts rate when the thermal injection is present and when it is blocked is $(1+\bar{n})$, giving the possibility of obtaining an absolute calibration of its intensity.

The mean photon number of the injected thermal state is also directly connected to the experimental homodyne quadrature distributions. The variance of the quadrature data for a thermal state is $V_{\rm th} = (1 + 2\bar{n}\eta)/4$, where η is the homodyne detection efficiency. Since the variance for a

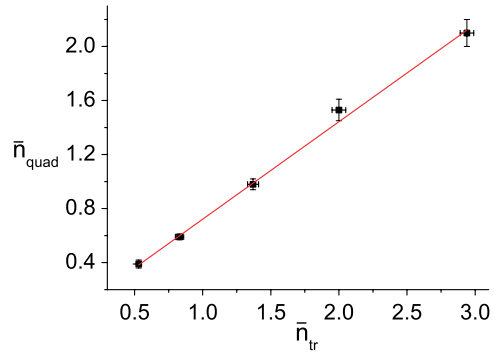

Figure 3. Plot of the mean number of photons in a thermal state as measured from the ratio of stimulated-to-spontaneous trigger counts ($\bar{n}_{tr}$) and from the variance of the homodyne quadrature measurements ($\bar{n}_{quad}$). A linear behaviour up to relatively high mean photon numbers is observed, which confirms a constant detection efficiency in the system.

vacuum state is $V_0 = 1/4$, by plotting $(V_{th}/V_0 - 1)/2$ versus the $\bar{n}$ values coming from the trigger counts one should obtain a linear dependence with the detection efficiency η as the proportionality factor. Increasing the mean photon number of the thermal state leads to widening the range of quadrature values that the homodyne detector has to analyse. Verifying the behaviour described above is a method to check the linearity of the response of our detector to large quadrature values. The test is shown in figure 3 for thermal states with a mean photon number ranging from $\bar{n} = 0.5$ to $\bar{n} \approx 3$ and the linear behaviour is clearly demonstrated.

2.2. *Single-photon subtraction*

Single-photon subtraction is experimentally implemented in a conditional way: a high-transmissivity beam splitter, BS, (here implemented with a half-wave plate followed by a polarizing beam splitter) is placed in the path of the light field and the quantum operation succeeds each time that an on/off detector fires in the reflected mode. It is straightforward to show that such a scheme is a very faithful implementation of the ideal single-mode photon annihilation operator $\hat{a}$ for states with low mean photon numbers and for low BS reflectivity [1]. In the case of a beam-splitter reflectivity of about 1% and also taking into account that the on/off detector is not able to discriminate between one photon or more [4], the fidelity between the state generated using the scheme described above and the ideal single photon subtraction is >98%.

When a single subtraction operation is needed, particular care has to be taken in order to perform the photon subtraction from exactly the right mode, i.e., from that probed by homodyne detection. To this purpose one has to carefully mode-match the reflection mode of the beam splitter to the LO mode; this is done by means of lenses and making use of a CW laser source for interferometrically precise alignment.

When the two subtraction operations are used for the proof of non-commutativity in the scheme of figure 1, it is necessary to make sure that both subtraction stages are equivalent. This is particularly important for the scheme proposed in [2], where the modes reflected by the two subtraction beam splitters have to be exactly matched in order to efficiently interfere. In both the subtraction stages the field in the reflected channel is collected by single-mode fibres identical to that, which defines the thermal mode; the two fibres are then connected to on/off detectors.

While the reflected mode in the second subtraction stage is carefully matched to the local oscillator mode, the reflected mode in the first subtraction stage is matched to the mode of the seed thermal field. In the first case, photon subtraction is performed in the LO mode: this roughly means that there may be a portion of the input thermal state that does not undergo photon subtraction, but this part is not seen by the homodyne detection performed in the LO mode. In the second case, the whole thermal state undergoes photon subtraction, but only the part of the photon-subtracted thermal state that is in the LO mode is efficiently detected. The two processes are indeed equivalent; this can be shown noting that the procedure $\hat{a}\,\mathrm{tr}_2\,\{\hat{B}^\dagger\hat{\rho}_{th}\,|0\rangle_{22}\,\langle 0|\,\hat{B}\}\hat{a}^\dagger$ (first loss of a thermal portion and then subtraction) is equivalent to $\mathrm{tr}_2\{\hat{B}^\dagger(\hat{a}\hat{\rho}_{th}\,\hat{a}^\dagger)\,|0\rangle_{22}\,\langle 0|\,\hat{B}\}$ (first subtraction and then loss of a state portion). The two lead in fact to the same final state. To be noted that these losses, described by the BS operation $\mathrm{tr}_2\{\hat{B}^\dagger\hat{\rho}\,|0\rangle_{22}\,\langle 0|\,\hat{B}\}$ do not enter in the analysis as detection or preparation losses, because homodyne analysis only sees the portion of the field in the LO mode.

The equivalence between the two subtraction stages was also experimentally verified by comparing the final states resulting from the two stages of photon subtraction when the same thermal state is fed as the seed. Figure 4 shows the measured homodyne quadrature distributions for the two cases and the corresponding reconstructed photon number probability distributions.

The reconstructed Wigner functions for the thermal state and its photon-subtracted versions obtained in the first and second subtraction stages are also reported in figure 5.

2.3. *Thermal states and their temporal characterization*

All above considerations imply the use of thermal states as the input field in the chain of quantum operations. However, real thermal states with a non-negligible mean number of photons in a highly localized spatiotemporal mode are difficult to produce. For this reason we adopted a rather popular trick to generate pseudo-thermal states of light with a nice Gaussian single spatial mode and the same spectral/temporal width of the local oscillator used to analyse them. A rotating ground glass disc (RD) is inserted in the coherent laser beam, and the scattered light forms a random spatial distribution of speckles. A single-mode fibre is placed in front of the wheel to collect a portion of the scattered light and select a clean single-spatial-mode beam for seeding the SPDC crystal. If the speckle average size is larger than the core diameter of the fibre, then only a single speckle contributes and, if the wheel is kept still, a coherent beam exits the fibre for SPDC injection (see figure 6(A)). However, when the ground glass disc rotates, the contributions of different speckles with random amplitudes and phases rapidly mix up (see figure 6(B)), and light exits the fibre yielding the photon distribution typical of a thermal

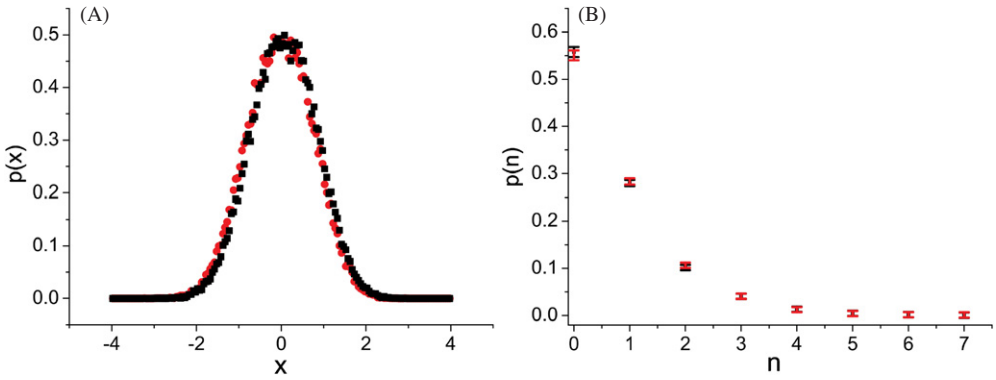

Figure 4. Quadrature distributions (A) and reconstructed diagonal density matrix elements (B) for the single-photon-subtracted thermal state obtained in the first (red circles) and in the second (black squares) subtraction stages.

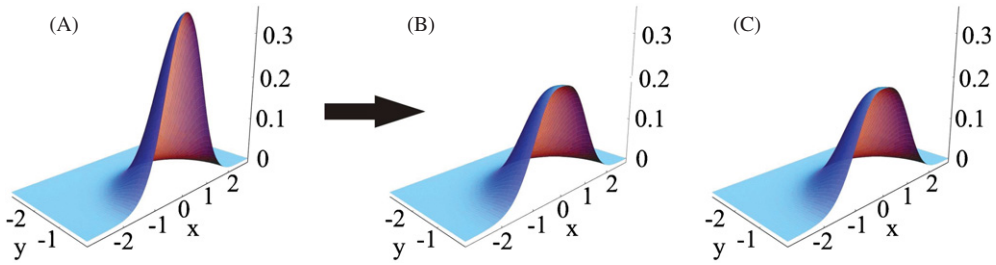

Figure 5. Experimentally reconstructed Wigner functions for (A) thermal state, (B) photon-subtracted thermal state before the photon-addition stage and (C) photon-subtracted thermal state after the photon-addition stage.

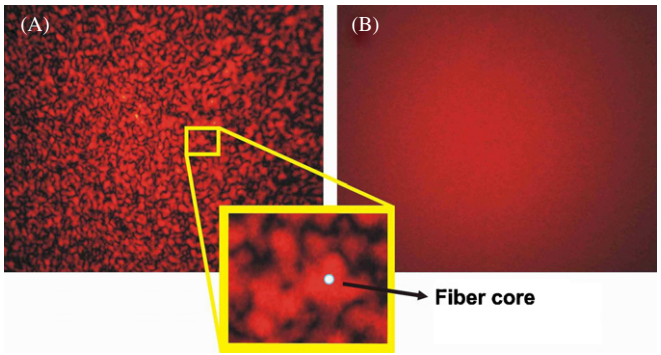

Figure 6. Speckle spatial distribution when the ground glass disc is at rest (A) and when it is moving (B). The inset shows a small portion of the speckle pattern and the approximate relative size of the single-mode fibre core.

source [29], but still in a clean, collimated, spatial mode. Indeed, this experimental realization of a thermal state directly recalls its P-function definition, i.e., a statistical mixture of coherent states weighted by a Gaussian distribution. The mean photon number of this thermal state can be adjusted by varying the intensity of the impinging beam on the rotating disc by means of a variable neutral density filter (VF).

It is important to note at this point that successive measurements on uncorrelated coherent states are only performed if the rate at which the different speckles cross the fibre core is high enough. If the pulse repetition and homodyne acquisition rate is of the same order of this, then successive measurements are performed on coherent states with little or no difference in amplitude and phase since they derive from the same speckle at the fibre input. The resulting quadrature measurements will thus show some degree of correlation depending on the ratio between the two rates.

The speckle crossing time, directly linked to the coherence time of the generated pseudo-thermal states, can be readily adjusted by varying the size of the speckles (changing the size of the laser spot on the glass disc or the distance between the disc and the fibre tip) and the disc rotation speed. However, even in the best experimental conditions, the shortest coherence times we obtained were of the order of fractions of a microsecond. If measurements are performed at the full repetition rate of the laser pulse train (82 MHz), the time separation between successive acquisitions (about 12 ns) is much shorter than the coherence time of the thermal state and significant correlations are to be expected among each pulse and the surrounding ones.

A clear indication of this behaviour is illustrated in figures 7, where quadrature measurements x_i for a given ith pulse are correlated to quadrature measurements x_{i+j} for the $(i+j)$th pulse, in the three cases of $j = 2, 15, 30$. It is evident that correlations are very significant for close neighbours whereas they tend to disappear for distant pulses.

A more complete analysis can be performed by measuring the correlation coefficient calculated as

$$\sum_i (x_i - \bar{x})(x_{i+j} - \bar{x}) \times \left(\sqrt{\sum_i (x_i - \bar{x})^2} \sqrt{\sum_i (x_{i+j} - \bar{x})^2} \right)^{-1}, \quad (1)$$

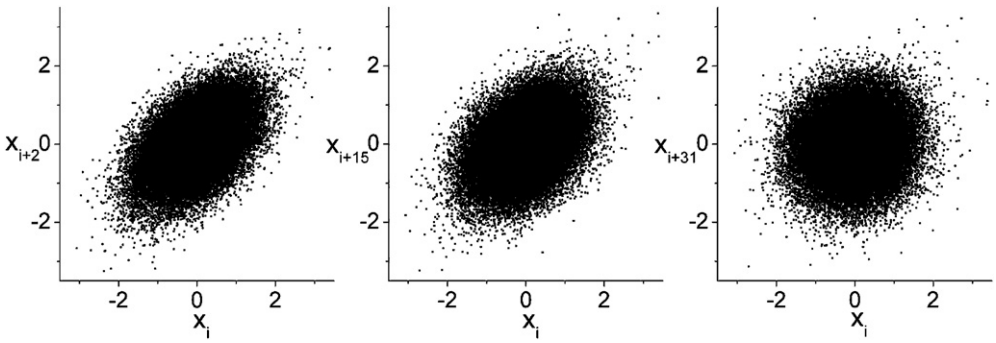

Figure 7. *XY* plots correlating quadrature measurements on pulses i and $i + j$, for $j = 2, 15, 30$, of a pseudo-thermal state pulse train. A clear correlation appears between nearby pulses, due to the finite coherence time of the state that is longer than the interval between successive pulses.

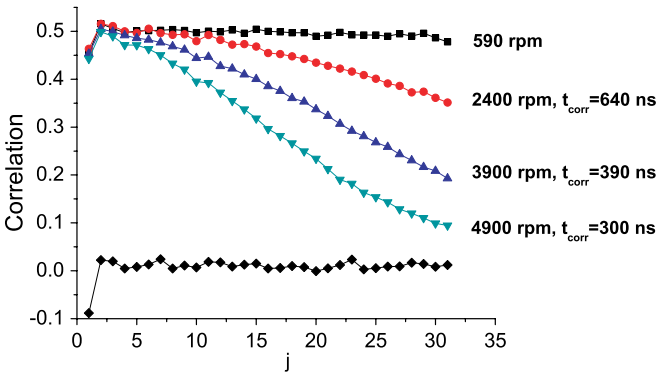

Figure 8. Correlation coefficient of quadrature measurements between each ith pulse and the successive $(i + j)$th ones (with $j = 1, \ldots, 30$) for different disc rotation speeds. The lowest curve corresponds to the case of a vacuum state.

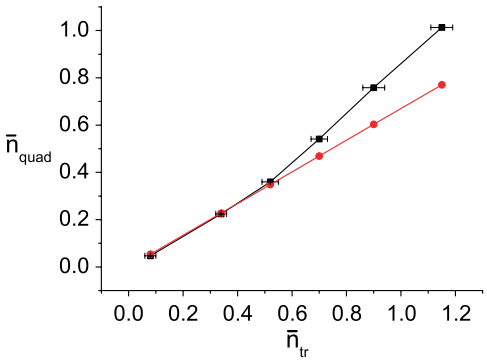

Figure 9. Same as figure 3 but with the quadrature measurements performed on the second pulse after an addition or subtraction event. Linearity is lost due to the correlations between successive quadrature measurements.

as a function of j for different disc rotation speeds (see figure 8). The higher the rotation speed, the shorter the coherence time of the generated thermal state, and the faster the decay in correlations between successive pulses. Note that this kind of measurements is effectively equivalent to measuring the $G^{(1)}(\tau)$ linear correlation function of the field. Plots in figures 7 correspond to the lower curve of figure 8, taken at the maximum rotation speed (about 5000 rpm) allowed in our experimental setup. Figure 8 also shows correlation data for successive quadrature measurements of a vacuum state, simply obtained by blocking the signal input to the homodyne detector. In this case, successive measurements are seen to be completely uncorrelated, apart for a small anti-correlation between each pulse and the immediate neighbour. This effect is connected to the finite bandwidth of the homodyne detector (see [18]) and is also present in the thermal state measurements, where it slightly reduces the correlation coefficient for $j = 1$.

From the above considerations, it should be evident that particular care has to be taken when acquiring and analysing homodyne data for pseudo-thermal states at very short timescales. However, what we are mainly interested in is the generation and analysis of photon-added and -subtracted thermal states that are produced and analysed at much lower rates. Indeed, if the state preparation rate is smaller than the inverse coherence time of the state, then each single-photon operation is performed on a coherent state having an amplitude and phase which are completely uncorrelated with respect to those of the previous one. Both single-photon-addition and -subtraction events in our experiments took place at maximum rates of the order of 1 kHz, to be compared to typical coherence times of about 1 μs. No correlation is thus expected to survive in these conditions.

A final point should be taken into account when dealing with the analysis of pseudo-thermal states. In most of our previous experiments the acquisition of homodyne data triggered by on/off photodetection events took place for two successive pulses of the LO train. The first one was coincident with the trigger event and contained the desired state information, while the second was used for calibration purposes. In the case of single-photon Fock state generation, the first pulse 'contains' the single photon, while the next one just 'contains' vacuum and is used for determining the scale of quadrature values. In principle, the same scheme could be used in the case of thermal states, where the pulse coincident with the trigger brings information about the photon-added or -subtracted state, while the second just contains the original state and can be used for a calibration of the mean number of photons in the seed thermal field. This can be done from an analysis of the quadrature distribution variance as discussed

above. However, due to the correlations between successive pulses, this scheme cannot be safely applied here. This is evident when plotting the mean photon numbers obtained from the quadrature variance analysis versus the mean photon numbers obtained from the stimulated count rates. As shown above, there should be a linear relationship between the two, connected by the homodyne detection efficiency. In this case, in contrast, there is a clear departure from the linear behaviour for increasing mean photon numbers of the seed thermal state (see figure 9).

The reason for this behaviour is to be found in the fact that, due to the $\sqrt{n+1}$ or $\sqrt{n}$ in the expressions for the action of photon creation and annihilation operators on Fock states, the addition and subtraction of photons to/from a state is more likely to take place the higher the excitation already present. When applied to a mixture of coherent states, $\hat{a}^\dagger$ and $\hat{a}$ preferentially operate on those with higher mean number of photons. Due to the strong correlations between successive pulses in our setup, the second pulse after an addition or subtraction event is therefore not representative of the original thermal state, but rather of a higher temperature subset. Valid quadrature statistics for the seed thermal state can be extracted only by taking pulses sufficiently distant (more than one coherence time apart) from the conditioning ones or, better, by taking quadrature data at a reduced rate and without conditioning (this is the approach used for the measurements reported in figure 3).

3. Conclusions

The reliable experimental implementation of single-photon creation and annihilation operators has recently allowed researchers to perform fundamental tests of quantum mechanics and will soon give access to the complete control over quantum states of light for novel applications. In this paper, we have shown that such realizations can be very faithful and produce the desired action on a quantum state of light only when all experimental parameters are fully under control.

Acknowledgments

This work was partially supported by Ente Cassa di Risparmio di Firenze and by the CNR-RSTL initiative.

References

[1] Parigi V, Zavatta A, Kim M S and Bellini M 2007 Probing quantum commutation rules by addition and subtraction of single photons to/from a light field *Science* **317** 1890
[2] Kim M S, Jeong H, Zavatta A, Parigi V and Bellini M 2008 Scheme for proving the bosonic commutation relation using single-photon interference *Phys. Rev. Lett.* **101** 260401
[3] Zavatta A, Parigi V, Kim M S and Bellini M 2008 Subtracting photons from arbitrary light fields: experimental test of coherent state invariance by single-photon annihilation *New J. Phys.* **10** 123006
[4] Kim M S 2008 Recent developments in photon-level operations on travelling light fields *J. Phys. B: At. Mol. Opt. Phys.* **41** 133001
[5] Zavatta A, Viciani S and Bellini M 2004 Quantum-to-classical transition with single-photon-added coherent states of light *Science* **306** 660
[6] Wenger Jerome, Tualle-Brouri Rosa and Grangier P 2004 Non-Gaussian statistics from individual pulses of squeezed light *Phys. Rev. Lett.* **92** 153601
[7] Ourjoumtsev A, Tualle-Brouri R, Laurat J and Grangier P 2006 Generating optical schrodinger kittens for quantum information processing *Science* **312** 83
[8] Neergaard-Nielsen J S, Melholt Nielsen B, Hettich C, Molmer K and Polzik E S 2006 Generation of a superposition of odd photon number states for quantum information networks *Phys. Rev. Lett.* **97** 083604
[9] Wakui K, Takahashi H, Furusawa A and Sasaki M 2007 Photon subtracted squeezed states generated with periodically poled $KTiOPO_4$ *Opt. Exp.* **15** 3568–74
[10] Adesso G, Dell'Anno F, De Siena S, Illuminati F and Souza L A M 2008 Heisenberg-limited estimation of losses with non-Gaussian states (arXiv:0807.3958v1)
[11] Opatrný T, Kurizki G and Welsch D -G 2000 Improvement on teleportation of continuous variables by photon subtraction via conditional measurement *Phys. Rev.* A **61** 032302
[12] Cochrane P T, Ralph T C and Milburn G J 2002 Teleportation improvement by conditional measurements on the two-mode squeezed vacuum *Phys. Rev.* A **65** 062306
[13] Olivares Stefano, Paris M G A and Rodolfo B 2003 Teleportation improvement by inconclusive photon subtraction *Phys. Rev.* A **67** 032314
[14] Cerf N J, Krüger O, Navez P, Werner R F and Wolf M M 2005 Non-Gaussian cloning of quantum coherent states is optimal *Phys. Rev. Lett.* **95** 070501
[15] Eisert J, Scheel S and Plenio M B 2002 Distilling Gaussian states with Gaussian operations is impossible *Phys. Rev. Lett.* **89** 137903
[16] Giedke G and Ignacio Cirac I J 2002 Characterization of Gaussian operations and distillation of Gaussian states *Phys. Rev.* A **66** 032316
[17] Ramazza P L, Ducci S, Zavatta A, Bellini M and Arecchi F T 2002 Second-harmonic generation from a picosecond Ti:Sa laser in lbo: conversion efficiency and spatial properties *Appl. Phys.* B **75** 53
[18] Zavatta A, Bellini M, Ramazza P L, Marin F and Arecchi F T 2002 Time-domain analysis of quantum states of light: noise characterization and homodyne tomography *J. Opt. Soc. Am.* B **19** 1189
[19] Zavatta A, Viciani S and Bellini M 2006 Non-classical field characterization by high-frequency, time-domain quantum homodyne tomography *Laser Phys. Lett.* **3** 3
[20] Banaszek K, D'Ariano G M, Paris M G A and Sacchi M F 1999 Maximum-likelihood estimation of the density matrix *Phys. Rev.* A **61** 010304
[21] Lvovsky A I 2004 Iterative maximum-likelihood reconstruction in quantum homodyne tomography *J. Opt. B: Quantum Semiclass. Opt.* **6** S556
[22] Hradil Z, Mogilevtsev D and Rehacek J 2006 Biased tomography schemes: an objective approach *Phys. Rev. Lett.* **96** 230401
[23] Agarwal G S and Tara K 1992 Nonclassical character of states exhibiting no squeezing or sub-Poissonian statistics *Phys. Rev.* A **46** 485
[24] Zavatta A, Viciani S and Bellini M 2004 Tomographic reconstruction of the single-photon Fock state by high-frequency homodyne detection *Phys. Rev.* A **70** 053821
[25] Zavatta A, Viciani S and Bellini M 2005 Single-photon excitation of a coherent state: catching the elementary step of stimulated light emission *Phys. Rev.* A **72** 023820
[26] Lvovsky A I, Hansen H, Aichele T, Benson O, Mlynek J and Schiller S 2001 Quantum state reconstruction of the

single-photon Fock state *Phys. Rev. Lett.* **87** 050402
[27] Zavatta A, Parigi V and Bellini M 2007 Experimental nonclassicality of single-photon-added thermal light states *Phys. Rev.* A **75** 052106
[28] Kiesel T, Vogel W, Parigi V, Zavatta A and Bellini M 2008 Experimental determination of a nonclassical Glauber–Sudarshan p-function *Phys. Rev.* A **78** 021804
[29] Arecchi F T 1965 Measurement of the statistical distribution of Gaussian and laser sources *Phys. Rev. Lett.* **15** 912